Acta Crystallographica Section F
Structural Biology and Crystallization Communications
ISSN 1744-3091

Efficient UV detection of protein crystals enabled by fluorescence excitation at wavelengths longer than 300 nm

Karsten Dierks,[a]‡ Arne Meyer,[a]‡ Dominik Oberthür,[a] Gert Rapp,[b] Howard Einspahr[c] and Christian Betzel[a]*

[a]Institute of Biochemistry and Molecular Biology, University of Hamburg, c/o DESY, Notkestrasse 85, Building 22a, 22603 Hamburg, Germany, [b]Rapp OptoElectronic GmbH, Gehlenkamp 9a, 22559 Hamburg, Germany, and [c]PO Box 6483, Lawrenceville, New Jersey 08648-0483, USA

‡ Present address: Institute of Biochemistry, Laboratory for Structural Biology of Infection and Inflammation, University of Lübeck, c/o DESY, Build. 22a, Notkestr. 85, 22603 Hamburg, Germany.

Correspondence e-mail: christian.betzel@uni-hamburg.de

Received 12 November 2009
Accepted 24 February 2010

© 2010 International Union of Crystallography
All rights reserved

It is well known that most proteins and many other biomolecules fluoresce when illuminated with UV radiation, but it is also commonly accepted that utilizing this property to detect protein crystals in crystallization setups is limited by the opacity of the materials used to contain and seal them. For proteins, this fluorescence property arises primarily from the presence of tryptophan residues in the sequence. Studies of protein crystallization results in a variety of setup configurations show that the opacity of the containment hardware can be overcome at longer excitation wavelengths, where typical hardware materials are more transparent in the UV, by the use of a powerful UV-light source that is effective in excitation even though not at the maximum of the excitation response. The results show that under these circumstances UV evaluation of crystallization trials and detection of biomolecular crystals in them is not limited by the hardware used. It is similarly true that a deficiency in tryptophan or another fluorescent component that limits the use of UV light for these purposes can be effectively overcome by the addition of fluorescent prostheses that bind to the biomolecule under study. The measurements for these studies were made with a device consisting of a potent UV-light source and a detection system specially adapted (i) to be tunable *via* a motorized and software-controlled absorption-filter system and (ii) to convey the excitation light to the droplet or capillary hosting the crystallization experiment by quartz-fibre light guides.

1. Introduction

The preparation of crystalline samples for structural biology is greatly accelerated when a rapid, reliable and non-invasive method for detecting protein crystals and eliminating nonprotein crystals is available. This is especially true for the high-throughput methods of crystallization that are now in use in many laboratories (Echalier *et al.*, 2004). The utility of UV fluorescence for these purposes has been known in principle for many years (Asanov *et al.*, 2001; Bourgeois *et al.*, 2002), but its application by means of a practical system has only recently become available for standard laboratory use. In the past, a practical system for *in situ* detection would have required expensive optical equipment (DeLucas & Bray, 2004). For present-day applications in high-throughput crystallization setups (Chayen & Saridakis, 2002; Stevens, 2000; Blundell *et al.*, 2002; Hui & Edwards, 2003) there is the additional requirement that the detection device fits conveniently into established equipment (Judge *et al.*, 2005).

Absorbance of UV light by proteins predominantly arises from the presence of the amino acid tryptophan, which has an absorption band in the range 260–310 nm (Fig. 1) with a maximum at 280 nm (Voet & Voet, 1995). Tyrosine and phenylalanine also absorb in this range, but not nearly as strongly as tryptophan. Emitted fluorescence light is detected from approximately 300 to 450 nm, with an emission maximum at the blue edge of the visible spectrum of 340–360 nm (Lakowicz, 1999; Permyakov, 1993; see supplementary material). However, in most vapour-diffusion experiments the wells containing the protein solution and the precipitant reservoir are sealed by thin transparent polymer-film or glass cover slips. Unfortunately, as has been documented many times, materials such as glass and many polymers are less transparent for wavelengths in the energy region

Table 1
Protein crystallization conditions.

Protein	Provider/source	Method	Volume (µl)	Protein concentration in buffer	Precipitant volume (µl)	Precipitant
Lysozyme	Sigma/*Gallus gallus*	Hanging drop	3	20 mg ml^{-1} in 50 m*M* NaOAc pH 4.5	3	0.7 *M* NaCl in 50 m*M* NaOAc pH 4.5
Thaumatin (crystals after ∼2 d)	Sigma/*Thaumatococcus daniellii*	Hanging drop	4	40 mg ml^{-1} in 0.1 *M* Tris base pH 6.8	4	0.67 *M* disodium tartrate in 0.1 *M* Tris base pH 6.8
Glucose isomerase	Hampton Research/ *Streptomyces rubiginosus*	Hanging drop	3	30 mg ml^{-1} in 10 m*M* Tris–HCl, 5 m*M* $MgCl_2$ pH 8.0	3	1.9 *M* ammonium sulfate in 10 m*M* Tris–HCl, 5 m*M* $MgCl_2$ pH 8.0
Mistletoe lectin I	Author-isolated/*Viscum album*	Hanging drop	2	4 mg ml^{-1} in 0.2 *M* glycine–HCl pH 2.5	2	1.1 *M* ammonium sulfate in 0.2 *M* glycine–HCl pH 2.5

(<300 nm) that excites proteins to emit fluorescence light (Scholz, 1991). This opacity continues to be accepted as a limitation to the utility of UV fluorescence for routine evaluation of crystallization trials and has led to a number of novel approaches to the detection and verification of protein crystals, as underscored by recent articles in this journal (Gill, 2010; Raghunathan & Arvidson, 2010). On the other hand, it has also been shown that most proteins and many other biomolecules show intrinsic fluorescence when illuminated with a filtered mercury arc lamp source (Tan *et al.*, 1995) and that this source is effective in the detection of protein crystals in crystallization setups (Judge *et al.*, 2005). We show here that this powerful source is effective because excitation takes place by wavelengths longer than 280 nm, the well known maximum for absorbance by tryptophan, and because glass cover slips and transparent film coverings show remarkably higher transmission rates at these longer wavelengths. We describe analyses of the excitation and fluorescence spectra of crystals and solutions of the proteins lysozyme, thaumatin, glucose isomerase and mistletoe lectin I. The evaluation of crystallization experiments with these proteins was carried out in multi-well plates and other hardware, where samples are typically small droplets with a volume of the order of 0.5–10 µl.

2. Materials and methods

Samples of lysozyme (Sigma–Aldrich, Taukirchen, Germany), thaumatin (Sigma–Aldrich, Taukirchen, Germany), glucose isomerase (Hampton Research, Aliso Viejo, California, USA) and ferritin (Sigma–Aldrich, Taukirchen, Germany) were purchased commercially. Mistletoe lectin I was isolated from the plant *Viscum album* as described previously (Franz *et al.*, 1981) and NADP dependent glycerinaldehyde-3-phosphate-dehydrogenase from *Kluyveromyces lactis*. These proteins were crystallized using the conditions listed in Table 1. Three different multi-well plates were used for the experiments: the Nextal QIA1 µplate (Qiagen; catalogue No. 132041), the Greiner 288 low-birefringence (lbr) plate (Greiner; catalogue No. 609820) and the Linbro 24 plate (Jena Bioscience; catalogue No. CPL-101). RNA-staining experiments were carried out using SYBR Gold staining solution (Uyeno *et al.*, 2004). The transparent sealing film we used was Greiner Bio-One AMPLIseal (catalogue No. 676040) and has a thickness of 0.5 mm. Glass cover slips with dimensions of 20 × 20 × 0.17 mm (obtained from Menzel-Gläser, Germany) were siliconized with silicone solution (Serva, Germany; catalogue No. 35130) by incubating the cover slips for 20 min in the solution and then drying them.

2.1. UV-fluorescence instrumentation

A variety of commercial instruments are now available for use in the analysis of UV fluorescence from crystallization trials. Our initial instrument for these analyses adapted an XtaLight-100 UV-light source (Nabitec GmbH, Lüneburg, Germany) to a computer-controlled CCD microscope system equipped with a motorized *XY* stage (Diversified Scientific Inc., Birmingham, USA), allowing easy access to all droplet positions in crystallization setups. The XtaLight-100 was specially designed for the observation of protein fluorescence, while the microscope system was designed for scanning the multi-well plates typically used in crystallization experiments, *e.g.* Linbro 24 plates or Nextal QIA1 µplates, and storing crystallization-evaluation data in a database. However, we also combined a standard laboratory microscope (SZX 12, Olympus, Japan) with the UV-light source. These adaptations (Fig. 1) included a white-light source and for our purposes images were typically taken with illumination within the visible region of the spectrum and subsequently with UV illumination. This required a fast and automated switching mechanism between white and UV light. The instrument was equipped with attenuators for both sources, so that a combination of both visible and UV lighting would be possible and so that damage to proteins sensitive to electromagnetic radiation in the relevant energy range could be minimized. Since direct guiding of light though the optical system of the microscope would necessitate expensive quartz lenses and additional optical components such as beam splitters and could prove awkward for some crystallization setups, illumination was made to bypass the microscope completely. In the case of UV light, this was performed by using an inclined beam (Fig. 1) and the light from the mercury arc lamp was guided to the sample by a quartz light-guide conduit. The spectral composition of the light could be varied by inserting filters in the light path. For excitation, we used a combination of a 390 nm short-pass filter (Filter 1; Rapp Optoelectronic, Hamburg, Germany) preliminary to a UV-permeable glass filter (Filter 2; UG-filters, Schott, Mainz, Germany), which performs the

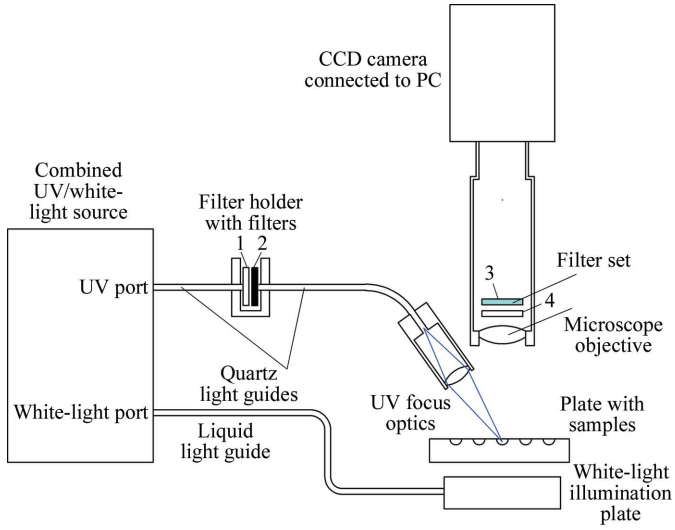

Figure 1
Schematic view of the instrumentation used. 1, short-pass filter (390 nm); 2, UG filter; 3, colour-compensation filter; 4, long-pass 400 nm filter.

main job of removing the visible part of the mercury arc lamp output. The 390 nm short-pass filter was introduced to reduce the amount of visible light incident on the primary UG filter, thereby protecting it from overheating from the intense light of the mercury arc lamp. A quartz lens was added to the source to focus the beam to a diameter of about 2 mm on the sample. A colour-compensation filter (Filter 3; Schott, BG 34) was inserted before the CCD camera to minimize artificial colour shift of images. In addition, a UV-blocking filter (Filter 4; long pass, 400 nm, Rapp Optoelectronic, Hamburg, Germany) was introduced to prevent excitation light entering the camera and to suppress the fluorescence of a filter (not shown) immediately in front of the CCD chip itself. Several features of this instrument are similar to those of the instrument described by Judge *et al.* (2005).

2.2. Fluorescence analysis

In order to estimate protein fluorescence intensities produced by illumination with the mercury arc lamp, we used a spectrophotometer to measure the emissions produced by monochromatic excitation of various amino acids. The fluorescence spectra of the amino acids are shown in Fig. 2. The aromatic tryptophan and tyrosine show relevant fluorescence when illuminated with UV light in the range 250–310 nm for tryptophan and 250–290 nm for tyrosine. Second excitation peaks with maxima at 220 nm for both amino acids are also observed, but they are irrelevant for UV detection of protein crystals because most materials used to contain crystallization trials are opaque to this part of the UV spectrum. The contribution of fluorescence of phenylalanine is insignificant and histidine shows no fluorescence at all. Obviously, the fluorescence of tryptophan can be excited with the longest wavelengths, but the efficiency of fluorescence excitation might be expected to be quite low for wavelengths greater than 300 nm. However, even wavelengths longer than 300 nm are effective in exciting fluorescence when the transmission properties of the most commonly used covering materials in protein-crystallization setups are considered.

2.3. Assaying transmission effects

The transmission spectra of glass cover slips, plastic films and the absorption of the glucose isomerase solution (Fig. 3*c*) were measured in a UV-Cuvette (Hellma; catalogue No. 105.252-QS) on a Cary 50 spectrophotometer (Varian, Palo Alto, California, USA). Here, the materials were placed in the optical path and the transmission spectrum was measured in the range 200–400 nm.

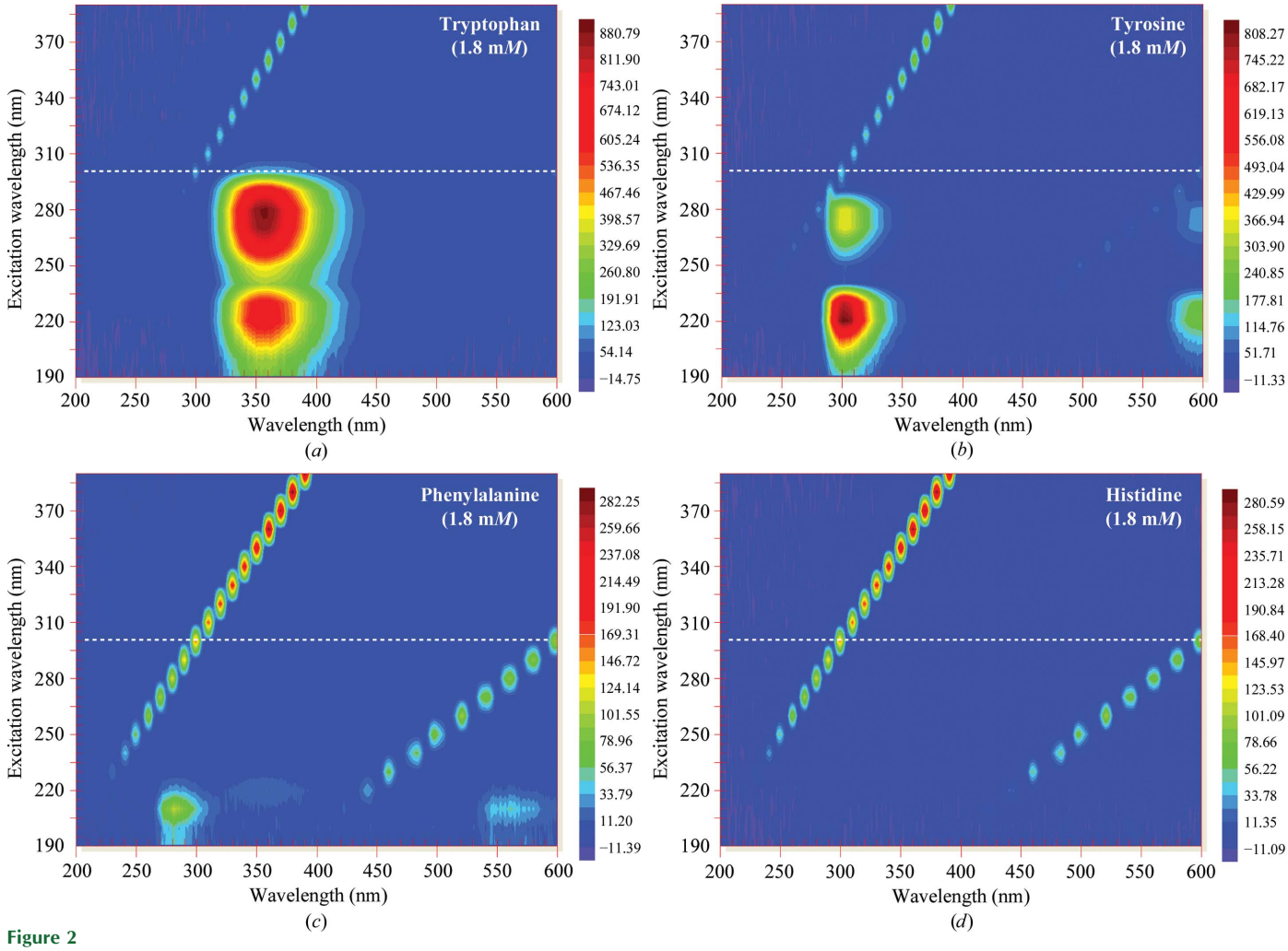

Figure 2
Two-dimensional diagram of amino-acid fluorescence. The sample solutions were placed in fluorescence cuvettes (Hellma; catalogue No. 105.252-QS). The fluorescence spectra were measured at discrete excitation wavelengths shifted in consecutive 5 nm steps from 190 to 390 nm using a Cary Eclipse fluorescence spectrophotometer. The relative fluorescence intensities are represented as a colour code.

To calculate the spectra effectively reaching the samples through either cover slips or plastic films, the lamp spectrum was corrected for the absorbance of the cover material. This was achieved by multiplying the filtered lamp spectrum by the measured transmission curve of the cover material step-by-step for each covering and was next corrected for absorption by the protein solution (passage through an estimated 0.5 mm of the initial protein concentration in the mixed droplet; Table 1) to give an estimate of the spectra incident on the crystal sample. The calculation process is illustrated in Fig. 3 and the impact on the absorption of four different proteins in solution and the fluorescence of one protein in the crystal is shown in Fig. 4.

3. Results

The illumination spectrum at the sample is the result of a combination of factors: the emission spectrum of the mercury arc lamp (see Fig. 2*a*), here called the source spectrum, the transmission spectra of the filters that modify the incident beam and the transmission spectra of the cover slips or film used to seal the crystallization chamber. The source spectrum is shown in Fig. 3(*a*) and the spectrum after passing the combined filters to remove radiation in the visible is shown in Fig. 3(*b*). The transmission spectra of siliconized cover slips and transparent film are shown in Fig. 3(*c*), which also shows the absorption spectrum of glucose isomerase for comparison. The overlap of the latter with the transmission spectrum of the film is robust, indicating that this film has good transmission properties. We have not attempted to evaluate all possible films available for this purpose and so cannot say whether all films are this transparent to UV light. In contrast, the overlap of the absorption spectrum of glucose isomerase with the transmission spectrum of the glass cover slip is much narrower and is centred roughly at 300 nm.

The resulting excitation spectra are shown on the left in Fig. 4 for samples under quartz cover slips (J&M, Analytische Mess & Regeltechnik GmbH, Aalen, Germany), plastic film and standard glass cover slips. The greatest reduction in incident excitation intensity is made by the glass cover slip. Fig. 4(*c*) also shows on the right the resulting fluorescence of a glucose isomerase crystal in a Nextal QIA1 µplate covered by different materials. The pictures show clearly that even if the crystal is covered with a glass cover slip unambiguous fluorescence can be observed at excitation wavelengths of 300 nm and longer. Radiation at 280 nm is almost completely absorbed by the cover slip and that at 290 nm is strongly absorbed, but radiation at 310 nm, while significantly attenuated, still retains about 30% of its original intensity.

Fig. 5 shows a comparison of images taken with UV and visible light of glucose isomerase, lysozyme, thaumatin and mistletoe lectin I crystallization setups in different multi-well plates under different covering materials. On the left side, a series of sitting drops is examined under both UV and visible light. These drops are in the Greiner and Nextal plates and are sealed by plastic film. The first two pairs show crystals that UV confirms to be protein. In the lower two pairs the UV image shows that the crystal is not protein.

On the right are a set of hanging drops viewed through glass cover slips. All of these are in Linbro plates. The top two UV images indicate that the crystals are proteins; in this case, thaumatin and mistletoe lectin I. The third pair show that the crystal seen in the visible is not protein. The UV image of this pair was taken before we realised the need to suppress the fluorescence from the CCD chip (filter 4, Fig. 1). The backlit image of the nonprotein crystal arises from a fortuitous reflection phenomenon caused by bright spots. The final pair on the right show that even under the most difficult conditions UV can indicate the presence of a protein crystal in an accumulation of nonprotein crystals.

Some biomolecules, *e.g.* proteins without tryptophan or nucleic acids, exhibit only weak fluorescence. In such cases marker substances may help to apply the methods described here (Kettenberger & Cramer, 2006). As an example, Fig. 6 shows crystals of an RNA nonamer stained with the nucleic acid-specific SYBR Gold (Invitrogen, Germany; catalogue No. S11494). The dye diffuses into the crystal and binds noncovalently to the RNA and as a result the crystal

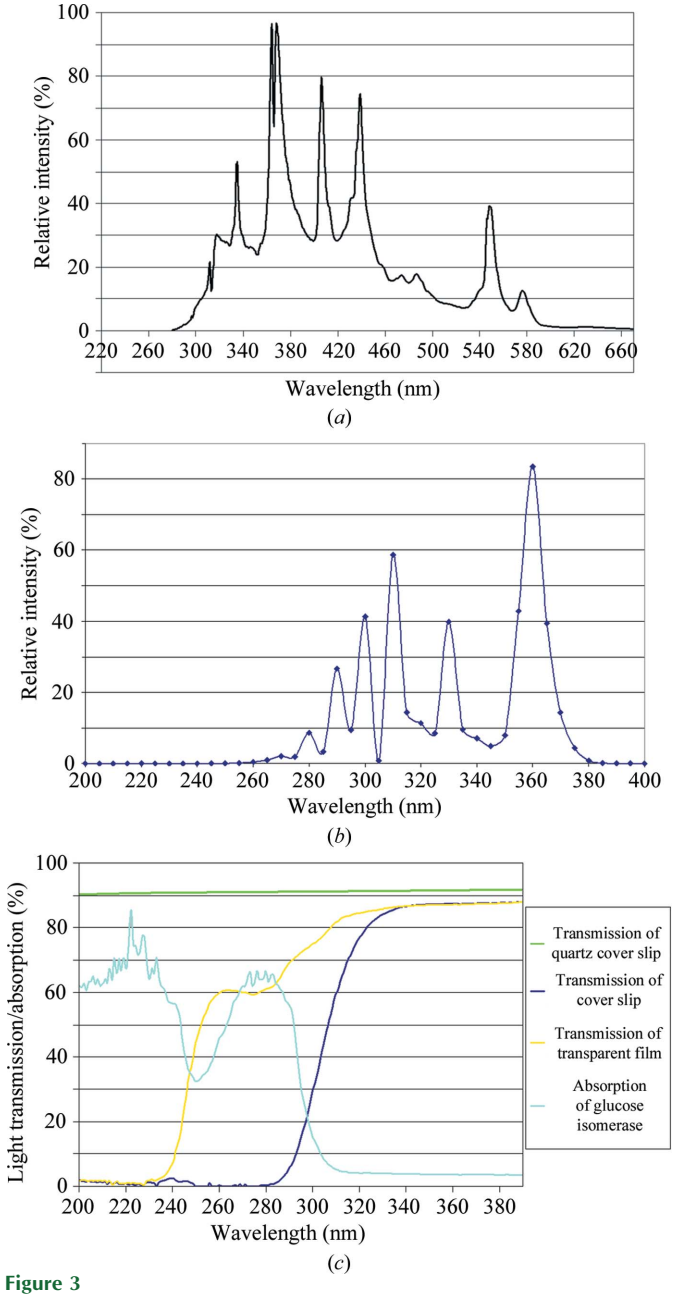

Figure 3
(*a*) Unfiltered product spectrum of the mercury arc lamp (HXP 120 W) as a light source as provided by its manufacturer (Osram). (*b*) Filtered emission spectrum of the system used to excite protein fluorescence, obtained by multiplication of the lamp spectrum by the transmission curves of the filters. (*c*) Transmission spectra of siliconized glass cover slips and transparent sealing film (Greiner Bio-One AMPLIseal). The absorption spectrum of glucose isomerase is shown for comparison. Light absorption of a glucose isomerase sample was measured with a Cary 50 spectrophotometer (Varian, Palo Alto, California, USA). It represents the typical absorption characteristics of a protein example.

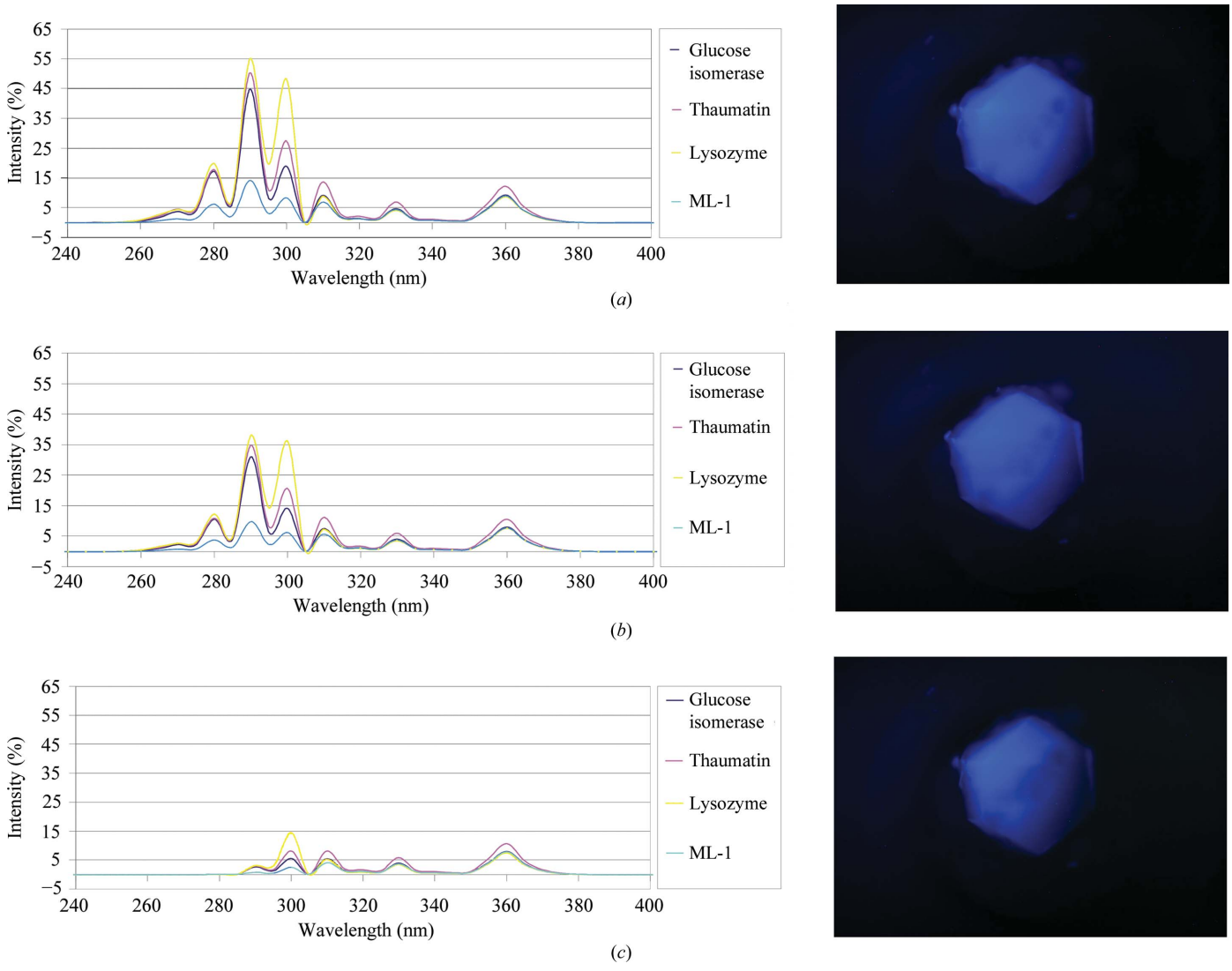

Figure 4
On the left, calculated effective UV excitation spectra for three different cover materials and for the same crystal of glucose isomerase are shown. On the right, fluorescence images collected with a CCD camera of a glucose isomerase crystal in a Nextal QIA1 µplate are shown when exciting with the spectra on the left. The exposure time was kept constant for all three cases to allow a 1:1 comparison. (*a*) The sample was covered with a quartz cover slip. (*b*) Sample covered with polymer film. The fluorescence of the crystal appears not to be degraded by use of the cover film, which can be understood by the similarity of the excitation spectra. (*c*) The sample was covered with a standard glass cover slip. Although the short wavelengths below about 300 nm are strongly absorbed by the cover slip, the fluorescence image is still remarkably clear. This is explained by the fact that even longer wavelengths are sufficiently effective to excite fluorescence. Note that, as explained in §2.3, the protein concentration varies between the four evaluated samples.

shows fluorescence caused by the incorporated dye. Reagents with similar properties, such as, for example, Bis-ANS or ANS (Groves *et al.*, 2007; Hawe *et al.*, 2008) and others (Raghunathan & Arvidson, 2010), are also available for protein fluorescence.

By variation of the illumination spectrum by the use of specific combinations of filters, even hard-to-detect protein crystals can be identified. After changing the excitation spectrum by inserting an additional short-pass filter (cutoff wavelength of <320 nm), strongly coloured ferritin crystals show intrinsic fluorescence (Supplementary Fig. 1). Moreover, the supplementary material[1] contains a variety of other illustrations of the utility of UV detection, including detecting protein crystals in amorphous precipitate and within glass capillaries.

[1] Supplementary material has been deposited in the IUCr electronic archive (Reference: GJ5077).

4. Discussion and conclusion

For the majority of the experiments described here the fluorescence of tryptophan was utilized to distinguish protein crystals from salt crystals and to detect protein crystals in both PEG and salt precipitations. The light-emission characteristics of the mercury arc lamp were used to overcome the lower absorption of proteins at wavelengths above 300 nm. The combination of the typically better transmission properties of the hardware for wavelengths above 300 nm together with the emission spectrum of the mercury arc lamp and the absorption properties of tryptophan yield clear detectable fluorescence that permits the detection of protein under difficult conditions and the unambiguous distinction of protein crystals from salt crystals and other artifacts by inspection.

During our experiments we also realised that the material that the multi-well plates are made of can show fluorescence of its own.

In addition, any residual protein in the mother liquor can fluoresce as well. Both effects can reduce the contrast of the fluorescence produced by the crystal. We note that the low-birefringence plates recently introduced by Greiner show a substantially reduced self-fluorescence when compared with most other standard plates made of polystyrene. Suitable fluorescence intensities have usually been obtained with exposure times in the range 1–10 s depending on the tryptophan content of the protein, the crystal size and the presence or absence of precipitation in the mother liquor. We have used two different standard colour camera types (QImaging QICAM 32-031B-176 Color, 12 bit and ImagingSource DFK41BF02.H, 8 bit) and obtained useful results. Our goal was to show that even with standard cameras UV detection of protein crystals is feasible without special adaptations of the optical system. Of course, performance may be improved by adapting lower signal-to-noise ratio cameras to this particular application, by adding enhancements such as cooling or by using a monochrome camera, but the point is that these measures are not necessary.

Finally, we note that UV light may trigger photochemical reactions. When illuminating proteins with UV light there is always some risk of damaging the proteins. To minimize this radiation damage, we focus the UV light only onto the droplet of interest and keep the exposure time to a minimum by only illuminating the droplet during the exposure time of the camera (typically about 1 s). Because switching

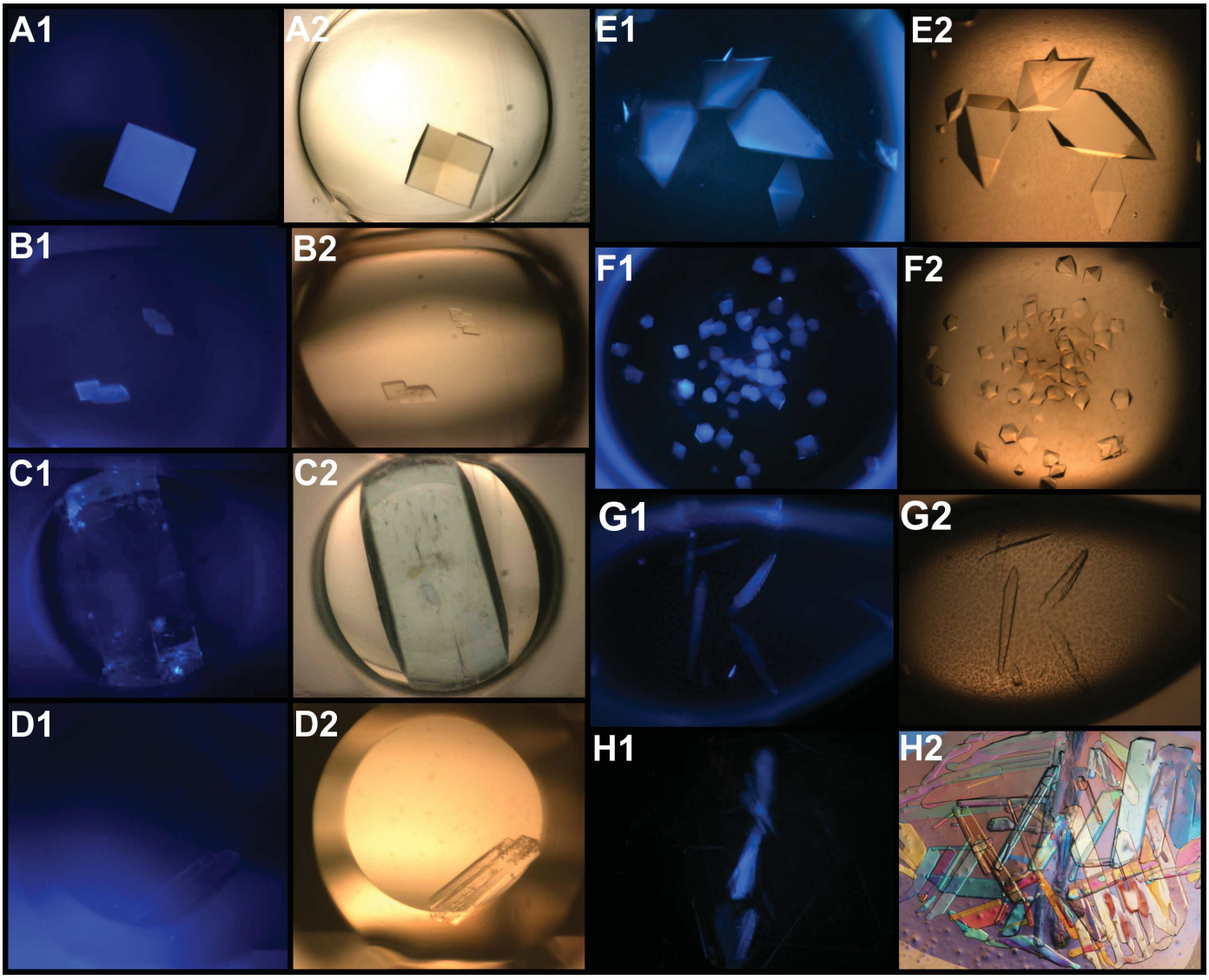

Figure 5
Examples of a variety of different protein and salt crystals in various plates under both white-light and UV illumination. A1–D2 are in sitting drops and E1–H2 are in hanging drops. A1, lysozyme crystal in a Greiner 288 low-birefringence (lbr) plate covered with transparent film and illuminated with UV light. A2, the same illuminated with white light. B1, a mistletoe lectin I crystal in a Greiner 288 lbr plate illuminated with UV light. B2, the same with white light. C1 and C2 show a potassium phosphate crystal in a Greiner 288 lbr plate illuminated with UV and white light, respectively. D1 and D2 show another example of a salt crystal in a Nextal QIA1 µplate illuminated with UV light and white light, respectively. E1, thaumatin crystals applying the hanging-drop method in a Linbro 24 plate covered with siliconized cover slips and illuminated with the filtered mercury arc lamp UV spectrum. E2, the same crystals illuminated with white light. F1, mistletoe lectin I crystals grown in hanging drops illuminated with UV light. F2, the same crystals illuminated with white light. G1, protein crystals of glycerinaldehyde-3-phosphate dehydrogenase grown in a hanging drop on a Linbro 24 plate illuminated with UV light. G2, the same crystals illuminated with white light. The drop contains 5.9%(*w*/*v*) PEG 4000 as precipitant in an acetate buffer. H1, a protein crystal underneath a shower of ammonium sulfate crystals that fluoresces under UV-light illumination but is invisible under polarized white-light illumination (H2). Without UV illumination, this protein crystal would most probably not have been detected.

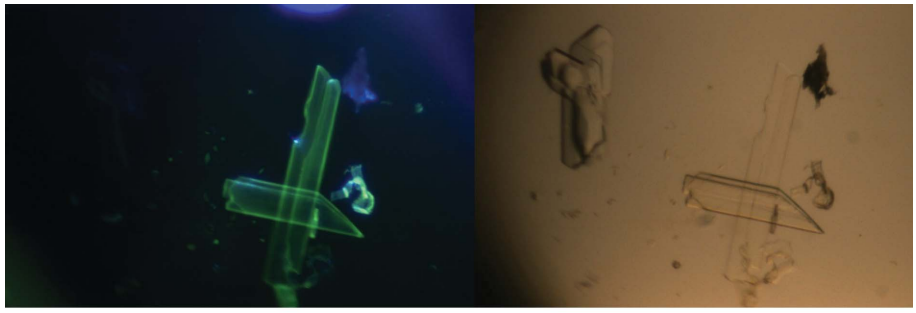

(*a*) (*b*)

Figure 6
Crystals of an RNA nonamer together with a sodium cacodylate crystal after adding the SYBR-Gold dye. (*a*) Illumination with UV light allows distinction between the salt crystal and the RNA crystal; (*b*) illumination with white light.

a mercury arc lamp on and off takes minutes, a shutter mechanism is used to obtain short exposure-time intervals. Nevertheless, the spectral range of 300–390 nm used to excite fluorescence normally causes less radiation damage compared with the shorter wavelengths around 280 nm (Pattison & Davies, 2006). If the excitation time is increased owing to poorer absorption efficiency of tryptophan or a below-average tryptophan content of the protein, the radiation damage should be expected to be comparatively less. Even so, we advise that fresh droplets, *i.e.* droplets in which crystals are still expected to grow, should not be irradiated with UV light because photoreactions may lead to unwanted effects such as aggregation.

The light source we used here can be adapted to many existing optical instruments, *e.g.* transmission microscopes, and even supersedes existing light sources in already established imaging systems by use of fibre optics. A combination of this instrument with a device that permits *in situ* dynamic light-scattering measurements in droplets has been described previously (Dierks *et al.*, 2008).

The work was supported by grants from the Deutsche Luft- und Raumfahrtagentur (DLR under Project No. 50WB0615) and the EU *via* the Network OptiCryst, LSHG-CT-2006-037793 (Contract No. 037793).

References

Asanov, A. N., McDonald, H. M., Oldham, P. B., Jedrzejas, M. J. & Wilson, W. W. (2001). *J. Cryst. Growth*, **232**, 603–609.
Blundell, T. L., Jhoti, H. & Abell, C. (2002). *Nature Rev. Drug Discov.* **1**, 45–54.
Bourgeois, D., Vernede, X., Adam, V., Fioravanti, E. & Ursby, T. (2002). *J. Appl. Cryst.* **35**, 319–326.
Chayen, N. E. & Saridakis, E. (2002). *Acta Cryst.* D**58**, 921–927.
DeLucas, L. J. & Bray, T. L. (2004). Patent WO/2004/005898 A1.
Dierks, K., Meyer, A., Einspahr, H. & Betzel, C. (2008). *Cryst. Growth Des.* **8**, 1628–1634.
Echalier, A., Glazer, R. L., Fülöp, V. & Geday, M. A. (2004). *Acta Cryst.* D**60**, 696–702.
Franz, H., Ziska, P. & Kindt, A. (1981). *Biochem. J.* **195**, 481–494.
Gill, H. S. (2010). *Acta Cryst.* F**66**, 364–372.
Groves, M. R., Müller, I. B., Kreplin, X. & Müller-Dieckmann, J. (2007). *Acta Cryst.* D**63**, 526–535.
Hawe, A., Sutter, M. & Jiskoot, W. (2008). *Pharm. Res.* **25**, 1487–1499.
Hui, R. & Edwards, A. (2003). *J. Struct. Biol.* **142**, 154–161.
Judge, R. A., Swift, K. & González, C. (2005). *Acta Cryst.* D**61**, 60–66.
Kettenberger, H. & Cramer, P. (2006). *Acta Cryst.* D**62**, 146–150.
Lakowicz, J. R. (1999). *Principles of Fluorescence Spectroscopy*, 2nd ed. New York: Springer.
Pattison, D. I. & Davies, M. J. (2006). *Cancer: Cell Structures, Carcinogens and Genomic Instability.* Basle: Birkhäuser Verlag.
Permyakov, E. A. (1993). *Luminescent Spectroscopy of Proteins.* Boca Raton: CRC Press.
Raghunathan, K. & Arvidson, D. N. (2010). Submitted.
Scholz, H. (1991). *Glass: Nature, Structure and Properties.* New York: Springer.
Stevens, R. C. (2000). *Curr. Opin. Struct. Biol.* **10**, 558–563.
Tan, W. H., Parpura, V., Haydon, P. G. & Yeung, E. S. (1995). *Anal. Chem.* **67**, 2575–2579.
Uyeno, Y., Sekiguchi, Y., Sunaga, A., Yoshida, H. & Kamagata, Y. (2004). *Appl. Environ. Microbiol.* **70**, 3650–3663.
Voet, D. & Voet, J. G. (1995). *Biochemistry*, 2nd ed. New York: John Wiley & Sons.